Oncogene (2016) **35**, 4580–4590

www.nature.com/onc

OPEN

ORIGINAL ARTICLE

Caspases uncouple p27^{Kip1} from cell cycle regulated degradation and abolish its ability to stimulate cell migration and invasion

SR Podmirseg[1], H Jäkel[1], GD Ranches[1], MK Kullmann[1], B Sohm[2,3], A Villunger[4,5], H Lindner[6] and L Hengst[1]

In addition to their role in programmed cell death, caspases exert non-lethal functions in diverse developmental processes including cell differentiation or tissue remodeling. Terminal cell cycle exit and differentiation can be promoted by increased level of the CDK inhibitor p27^{Kip1}. Activated caspases cause proteolytic processing of p27, and we identified a novel caspase cleavage site in human p27 that removes a C-terminal fragment of 22 amino acids from the CDK inhibitor, including a phosphodegron. Thereby, caspases protect the inhibitor from SCF-Skp2-mediated degradation in S, G2 and M phases of the cell cycle. As a consequence, p27 becomes stabilized and remains an efficient nuclear inhibitor of cell cycle progression. Besides controlling cyclin/CDK kinase activity, p27 also regulates cytoskeletal dynamics, cell motility and cell invasion. Following processing by caspases, p27 fails to bind to RhoA and to inhibit its activation, and thereby abolishes the ability of p27 to stimulate cell migration and invasion. We propose that the stabilization of the CDK inhibitor and elimination of RhoA-induced cytoskeletal remodeling upon caspase processing could contribute to cell cycle exit and cytoskeletal remodeling during non-lethal caspase controlled differentiation processes.

Oncogene (2016) **35,** 4580–4590; doi:10.1038/onc.2015.524; published online 1 February 2016

INTRODUCTION

The CDK inhibitor p27^{Kip1} controls cell proliferation by binding and regulating a broad range of cyclin-dependent kinases (CDKs).[1,2] A conserved N-terminal CDK-inhibitory domain is required and sufficient for CDK inactivation by Cip/Kip family proteins.[3] In addition to controlling cell cycle progression and cell cycle exit into quiescence,[1] CDK-independent functions of p27 have been established.[4] A mutant of p27 that fails to bind and regulate CDK complexes has oncogenic properties.[5] Upon export to the cytoplasm, p27 can regulate cytoskeleton dynamics, cell motility and cell invasion.[4,6–8] These functions depend on C-terminal domains of the protein.

Already shortly after its identification,[9–13] p27 was proposed to modulate apoptosis.[14,15] In multicellular organisms, apoptosis and the executing caspases are involved in the regulation of tissue homeostasis, development, the removal of damaged or infected cells,[16–19] differentiation and cancer development.[20] Interestingly, different molecular mechanisms have been proposed by which p27 may either promote or inhibit apoptosis. Expression of p27 delays DNA fragmentation and morphological changes associated with apoptosis,[21] whereas deletion or knockdown of p27 renders cells more susceptible to apoptosis.[15,22,23] Other reports find that overexpression of p27 can induce cell death[14] and p27 upregulation caused by treatment with various anticancer drugs can induce p27-dependent cell cycle arrest, followed by apoptosis.[24–26]

Proteases of the caspase family have a central role in the regulation of apoptosis,[16,27] but also exert non-lethal functions during development, inflammation, differentiation and tissue remodeling.[17–19,28] Proteolytic processing of p27 executed by caspases has been observed during apoptosis.[29,30] A potential cleavage site in human p27 was identified within a D^{136}PSD^{139}S consensus motif,[29] which would separate the nuclear localization signal (NLS) from the CDK-inhibitory domain. On the basis of this finding, it was expected that truncated p27 loses its ability to shuttle between cytosol and nucleus[31] and accumulates in the cytoplasm,[32,33] as it has been described for the closely related CDK inhibitor p21$^{Cip1/Waf1}$.[30,32] This could in turn relieve nuclear cyclin/CDK complexes from inhibition and promote apoptosis.[15,32,34] However, it was also observed that p27 can remain nuclear in apoptotic cells[30,32] and retains its ability to inactivate CDKs.[29] An inherent conundrum in either scenario is that caspase activation in most apoptosis paradigms follows mitochondrial outer membrane permeabilization that constitutes a point of no return in cell death signaling.[16,28,35] Limited caspase-mediated proteolysis of distinct substrates, however, has recently been reported in the context of death receptor activation, for example, upon ligation of the TNF, TRAIL or FAS receptors that can mediate cell survival, differentiation and promote inflammatory as well as migratory responses.[17–19,28,36]

In contrast to common believe, we now report that caspases do not cleave the human p27 protein at aspartate 139 (D139) *in vivo* or *in vitro*. Instead, we discovered a novel and conserved caspase consensus motif that leads to proteolytic processing of the CDK inhibitor at aspartate 176 (D176). Cleavage at this site fails to separate the NLS from the CDK-inhibitory domain, permitting nuclear import and CDK inhibition of caspase-processed p27. Caspase cleavage, however, removes the phosphodegron surrounding T187,[1,37,38] which leads to the stabilization of the truncated CDK inhibitor in S, G2 and M phases. In addition,

[1]Division of Medical Biochemistry; Biocenter; Innsbruck Medical University; Innsbruck, Austria; [2]Laboratoire Interdisciplinaire des Environnements Continentaux (LIEC), UMR 7360, Université de Lorraine, Metz, France; [3]CNRS, LIEC, UMR 7360, Metz, France; [4]Division of Developmental Immunology; Biocenter; Innsbruck Medical University; Innsbruck, Austria; [5]Tyrolean Cancer Research Institute, Innsbruck, Austria and [6]Division of Clinical Biochemistry; Biocenter; Innsbruck Medical University; Innsbruck, Austria. Correspondence: Professor L Hengst, Biocenter, Division of Medical Biochemistry, Innrain 80-82, Innsbruck A-6020, Austria.
E-mail: ludger.hengst@i-med.ac.at
Received 21 April 2015; revised 27 October 2015; accepted 6 November 2015; published online 1 February 2016

cleavage by caspases removes a domain of p27 that is required for the regulation of cell motility by binding to RhoA. We demonstrate that truncated p27 fails to bind RhoA and inhibit its activation. Consistent with this observation, caspase-processed p27 was unable to promote cell migration or cell invasion. Caspases[17,28] as well as p27[39–43] are regulating differentiation of various cell types. Using this novel mechanism, caspases and p27 could cooperate to induce a robust cell cycle exit, tissue remodeling and differentiation.

RESULTS

p27 is a caspase substrate *in vitro* and becomes processed upon caspase activation *in vivo*

The CDK inhibitor $p27^{Kip1}$ has been identified as a caspase substrate,[29,30,33] and a potential cleavage site was identified at the $D^{136}PSD^{139}S$ consensus motif in the human protein.[29] The serine residue in position 140 (S140) has recently been proposed as a phosphorylation site of p27.[44] As the residue following the cleavage site is a critical residue within caspase consensus motives, we speculated that phosphorylation might impair caspase processing.[45–47] To test this hypothesis, we generated a potentially phosphomimetic mutant by replacing serine residue 140 with glutamic acid. Purified recombinant p27 wild-type and the S140E mutant were incubated with recombinant caspase-3, and caspase-induced proteolysis was followed for 90 min. Surprisingly, the mutant protein was processed with similar efficiency as wild-type p27 (Figure 1a), indicating that the disruption of this proposed caspase consensus motif does not impair cleavage. We speculated that a different caspase consensus motif of p27 might be used or that a different protease might truncate p27 at this site in apoptotic cells. Such an enzyme might, for example, be 'KIPase', a protease with caspase-like activity that is part of the 20 S proteasome.[48,49]

Previously, processing of p27 by mulitple caspases (3, 6, 7 and 8) has been observed *in vitro*.[29,30] When apoptosis was induced by ultraviolet (UV) irradiation in WM35 melanoma cells, p27 was efficiently cleaved, following the activation of caspase-3 (Figure 1b). An induction of p27 protein level precedes the cleavage. This increase in protein level may be caused by the decline of the F-box protein Skp2, an ubiquitin ligase subunit that controls p27 stability.[1,38] The levels of cyclins D1, A and B1 declined, but cyclin E remained expressed and, as reported previously, the protein was also caspase-processed.[50]

The glucocorticoid analog dexamethasone initiates apoptosis in the human T-cell lymphoblast-like cell line CEM C7H2.[51] Dexamethasone is also used for the treatment of acute lymphoblastic leukemia. As in WM35 cells (Figure 1b), p27 levels were strongly induced during apoptosis (Figure 1c), whereas Skp2 level declined, as we recently described.[52] Again, a shorter form of p27 becomes readily detectable at the time of caspase-3 activation. This form co-migrates with the shorter form of p27 found in UV-treated WM35 cells (Figure 1c). To determine whether it also co-migrates with *in vitro* caspase-cleaved p27, the size of truncated p27 was compared with recombinant p27 that was incubated with caspase-3 (Figure 1c). The co-migration of all truncated forms in SDS–PAGE indicates that truncated p27 might be a product of caspase cleavage in intact cells. Since mutation of the proposed caspase consensus motif did not impair caspase processing *in vitro*, we decided to determine whether this or alternative sites become cleaved.

Caspases cleave p27 at amino-acid residue 176

In order to investigate if the product of *in vitro* caspase cleavage corresponds to the previously reported product (amino acids 1–139), we replaced the serine codon in position 140 by a stop codon and expressed the truncated protein in *Escherichia coli*.

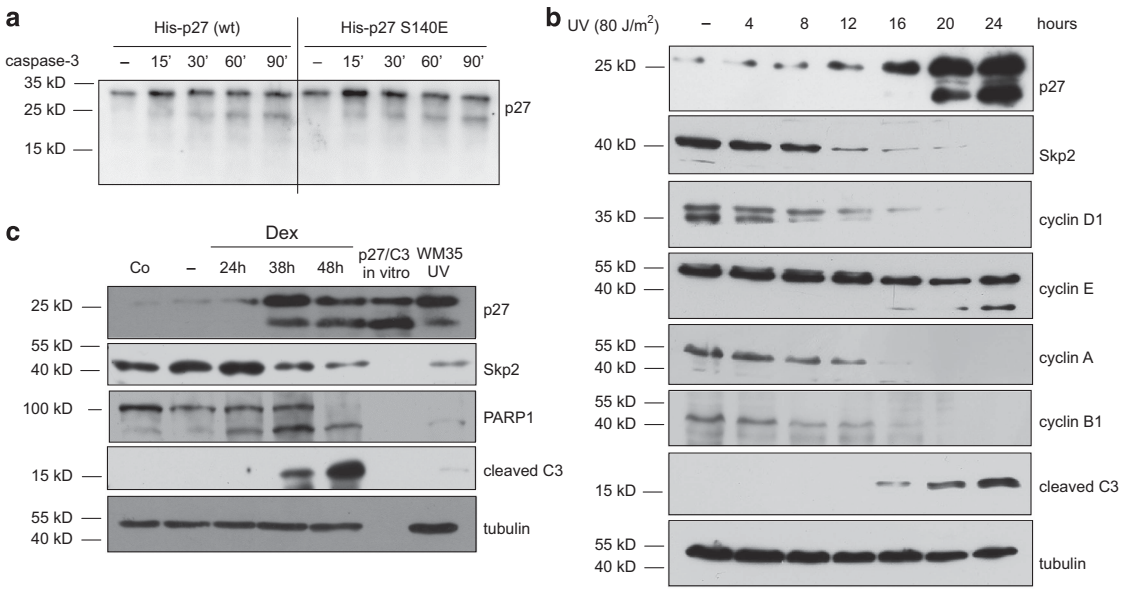

Figure 1. p27 is a substrate of caspases *in vitro* and *in vivo*. (**a**) *In vitro* cleavage of recombinant wild-type (wt) p27 and a p27-S140E mutant with caspase-3. Samples were taken from the reaction at the indicated time points and hexahistidine (His)-tagged p27 protein was detected by western blotting using anti-p27 antibodies. These antibodies detect the N-terminal fragment of the processing product. – represents recombinant p27 incubated in the absence of caspase-3 for 90 min. Representative blots of three independent biological experiments. (**b**) Apoptosis was induced in WM35 melanoma cells by irradiation with UV-light (80 J/m^2). Cells were collected at the indicated time points and extracts were separated by SDS–PAGE and analyzed for endogenous p27, Skp2, cyclin D1, cyclin E, cyclin A, cyclin B1, cleaved caspase-3 (C3) and β-tubulin. – indicates untreated cells. Representative blots of four independent biological experiments. (**c**) Apotosis was induced in CEM C7H2 cells by treatment with the glucocorticoid analogue dexamethasone (Dex) at a final concentration of 10^{-7} M. Cells were collected at the time points indicated and extracts were blotted for endogenous p27, Skp2, cleaved caspase-3, PARP1 and β-tubulin. p27 cleaved by caspase-3 *in vitro* and extract derived from UV-treated WM35 cells were loaded for size comparisons. Representative blots of three independent experiments are shown. (Co) represents a solvent (ethanol) control; – represents untreated cells.

The size of the truncated protein was compared with purified p27 that was cleaved by caspase-3 *in vitro*. The caspase-3 processed human p27 migrated significantly slower in SDS–PAGE than truncated p27 (1–139) (Figure 2a). Even after extended incubation, we failed to detect a fragment co-migrating with the p27 1–139 fragment. To identify potential caspase processing sites *in vitro* and *in vivo*, we mutated three aspartate residues present in minimal caspase consensus sequences at the C-terminus of p27. Mutations D139E or D159E failed to impair caspase cleavage *in vitro*. Only when aspartate 176 was mutated, human p27 was no longer cleaved by caspase-3 (Figure 2b). Importantly, the mutation D176E also prevented processing of overexpressed p27 in WM35 cells undergoing apoptosis after UV-induced DNA damage (Figure 2c). Truncated p27 co-migrates with a fragment of p27 including amino acids 1–176 (Figure 2c). To exclude that different caspases use different sites, we incubated purified human p27 as well as the D176E mutant with purified recombinant effector caspases 3 and 7 and the initiator caspases 2 and 8 (Figure 2d). Prior to the experiments, activities of these caspases were matched using specific fluorescent substrates. All caspases could process p27 but not the mutant D176E, and caspase-7 processed p27 most effectively (Figure 2d). To exclude potential contaminations with bacterial proteases, we incubated p27 in presence of a catalytic inactive mutant of caspase-2, which was purified following the same procedure as the active caspases. Incubation with the inactive mutant did not result in p27 cleavage, excluding such possibility (Figure 2d, lower panel).

To determine the caspase processing site in p27, the products of a caspase-3 *in vitro* cleavage reaction (Figure 3a) were subjected to mass spectrometric analysis using MALDI-TOF. p27 including its N-terminal methionine has a calculated molecular weight of 22 073 Da, but migrates at a significant larger size (27–28 kDa) in SDS–PAGE. If analyzed by mass spectrometry, purified bacterially expressed p27 had a molecular weight of 21 935 Da, which corresponds to full-length p27 lacking the N-terminal methionine (calculated molecular weight 21 942 Da; Figure 3b, upper panel). Following caspase processing, a second peak with smaller mass was detected (19 600 Da; Figure 3b, lower panel), in addition to the peak representing full-length p27 (21 948 Da). A number of potential internal p27 peptide sequences could theoretically fit to this peak. Only one of these sequences starts at the N-terminal serine following the initiator methionine and this fragment ends at aspartate residue 176 (Figure 3c). To confirm that the 19 600 Da fragment is this peptide and not an internal p27 fragment, we performed N-terminal sequencing of this fragment and found five amino acids following the start methionine (which is missing in the recombinant protein). This clearly identified the 2–176 N-terminal processing product of human p27 and demonstrated that caspases cleave p27 at aspartate D176.

The caspase motif that we have identified is highly conserved in p27 orthologs from mammalian species, whereas sequences surrounding D139 are less conserved (Figure 3d). Interestingly, p27 from human, rhesus monkey, chinese hamster or long-tail chinchilla lack a good caspase consensus motif preceding D139.

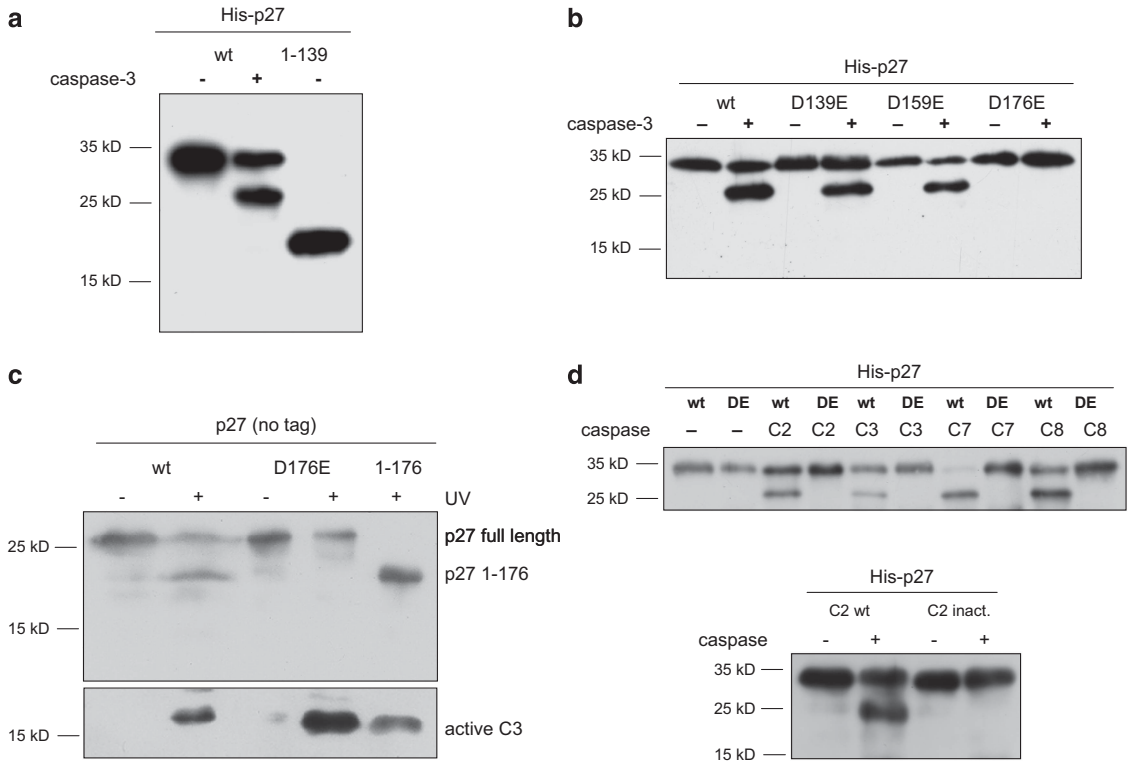

Figure 2. Caspases cleave p27 at residue 176 *in vivo* and *in vitro*. (**a**) SDS–PAGE analysis of *in vitro* caspase-3 processed recombinant N-terminal His-tagged p27 with recombinant N-terminal His-tagged p27 truncated at position 139. His-tagged proteins were detected by western blotting using antibodies directed against the N-terminal hexahistidine tag. (**b**) Recombinant His-tagged p27 wild-type (wt) protein as well as His-tagged mutant proteins (D139E, D159E, D176E) were subjected to caspase-3 cleavage *in vitro* followed by western blotting. (**c**) WM35 melanoma cells were transfected with untagged p27 wild-type, a D176E mutant of p27 and a mutant carrying a stop codon following aspartate 176 (1–176). Apoptosis was induced by irradiation with UV-light (80 J/m^2). Cells were collected 16 h after UV irradiation. Due to different expression levels, p27 levels have been matched before western blot analysis. One representative blot of 3 independent biological experiments is shown. (**d**) Recombinant His-tagged p27 wild-type and the D176E point mutant (DE) were incubated with the indicated caspases (caspases 2, 3, 7 and 8). p27 proteins were detected by western blotting. A control of recombinant caspase preparation is shown in the lower panel: Recombinant His-tagged p27 wild-type (wt) was incubated either with recombinant wild-type caspase-2 (wt) or an inactive mutant C326G (inact.).

This is due to the proline residue in position 137, which has been shown to break a caspase consensus site.[53,54] Interestingly, other mammalian species including mouse exhibit a caspase consensus sequence surrounding D139 (Figure 3d). To investigate p27 cleavage upon induced cell death in primary cells and to investigate caspase processing of murine p27, we used mouse primary thymocytes that are destined to die when grown in cell culture.[55] Cell death can even be accelerated by treatment with dexamethasone.[56] To characterize the size of p27 cleavage products that occur during apoptosis, we overexpressed murine p27 and fragments truncated at D176 or at D139 in mouse embryonic fibroblasts (MEFs). In apoptotic primary thymocytes, we detected a caspase cleavage product of endogenous p27 that comigrated with the fragment of murine p27-1–176 (Figure 3e). This confirmed that the novel cleavage fragment exists in primary cells and in mice. In addition to this fragment, mouse p27 is processed into a second fragment which co-migrates with the p27-1–139, suggesting that the second site is also used in mice (Figure 3e). This difference was also confirmed using purified recombinant human and mouse p27 *in vitro* (Figure 3f). Whereas the human protein is exclusively processed into the fragment 1–176, two fragments were obtained from the mouse protein (Figure 3f).

Compared to the shorter product, caspase cleavage fails to remove the NLS from the CDK-inhibitory domain (Figure 3g). Cleavage of p27 will, however, remove two important phosphorylation sites that control the cell-cycle-dependent stability of p27.[1,57] The loss of the SCF-Skp2 ubiquitin ligase recognition motif might render p27 stability independent from CDK activities and cell cycle positioning. Phosphorylation at residue T198 stabilizes the CDK inhibitor in early G1 and promotes its cytosolic localization,[1,58] and deletion of T198 or the loss of the surrounding region stabilizes p27.[58,59] Therefore, truncation of the C-terminus may permit a cell cycle phase-independent accumulation of p27, by disrupting two important pathways of p27 degradation.

Caspase-processed p27 remains an inhibitor of nuclear CDKs and is stabilized in S, G2 and M phases of the cell cycle

It was previously suggested that cleavage of p27 by caspases generates a protein that cannot be imported in the nucleus and therefore fails to inhibit nuclear cyclin/CDK complexes.[30,32,33] As the NLS is still present in the large fragment of caspase-cleaved p27 (Figure 3g), we wished to determine whether the product of caspase processing remains nuclear. Immunofluorescence analysis of HeLa cells transfected with Flag-tagged proteins revealed that truncated p27 predominantly localized in the nucleus, similar to the full-length protein. In contrast, the earlier described fragment ending at residue 139 was located throughout the cell (Figure 4a). To confirm the distribution of p27 in apoptotic cells, we fractionated WM35 melanoma cells induced to undergo apoptosis by UV irradiation (Figure 4b). Both, p27 and the truncated p27 were found in the nuclear fraction. The finding that endogenous cleaved p27 remains nuclear is consistent with some earlier observations.[29]

We also determined whether the truncated fragment of human p27 still binds cyclin/CDK complexes. Cyclin E remains expressed in apoptotic WM35 cells (Figure 1b). We precipitated endogenous cyclin E from apoptotic cells and analyzed the presence of full-length and truncated p27 in the immune complexes. Endogenous full-length and truncated p27 were in complex with cyclin E in apoptotic cells (Figure 4c).

Previous studies reported that p27 binding to CDK2 complexes is reduced during apoptosis.[30] We investigated the ability of cleaved p27 to act as a CDK inhibitor *in vivo* in HEK 293T cells and immortalized $p27^{-/-}$ MEFs. When overexpressed in 293T cells, p27 as well as the truncated form induced a strong accumulation of cells in G1 phase (Supplementary Figure 1a). To investigate cell cycle regulation at expression level close to the endogenous protein, we used lentivirally transduced $p27^{-/-}$ MEFs. Expression level did not severely exceed that of endogenous p27 in wild-type MEFs (Figure 4d). Cell cycle profiles revealed that moderate overexpression of full-length but also truncated human p27 slightly increased the percentage of cells in G1 phase and decreased cells in S phase, suggesting that the CDK-inhibitory potency of these proteins is similar *in vivo* (Figure 4e). Despite of being expressed at higher levels (Figure 4d), which may stem from loss of feedback regulation,[1,60] human p27 mutants deficient for cyclin/CDK complex binding (CK^-)[61] used as controls had no effect on cell cycle distribution.

p27 is stable in early G1 phase and becomes unstable upon CDK activation at the restriction point.[1,38] Efficient proteasomal degradation of p27 in S/G2 phase results from its phosphorylation at T187 and subsequent ubiquitination by the SCF-Skp2 ubiquitin E3 ligase. Deletion of the C-terminal phosphodegron could stabilize p27 in S, G2 and M phase. In order to investigate the stability of truncated p27 in different cell cycle phases, we treated HeLa T-REx cells that conditionally express p27 full-length or p27-1-176 with lovastatin (G1 arrest), thymidine (S phase arrest) or nocodazole (G2/M arrest). The expression of the different p27 mutants was subsequently induced in arrested cells. Even in asynchronous cells, the wild-type protein was expressed at lower levels than the truncated form 1–176 (Figure 4f). Both proteins were stable in lovastatin-arrested cells, where Skp2 levels are low.[62] In thymidine-arrested cells, p27 is unstable due to SCF-Skp2-dependent degradation. However, the p27-1-176 mutant was stable in thymidine-arrested cells, as was a p27-T187A point mutant lacking the Skp2-specific phosphodegron (Supplementary Figure 1b). Compared with wild-type p27, the p27-1–176 mutant was also stabilized in nocodazole-arrested cells (Figure 4f).

Truncated p27 does no longer bind or inhibit RhoA

A CDK-independent function of p27 is the regulation of cytoskeleton dynamics. The C-terminal domain of p27 interacts with the small GTPase RhoA and inhibits its binding to guanine exchange factors.[63] This prevents the activation of the GTPase and influences the formation of stress fibers and cell motility. Interestingly, phosphorylation of p27 on the very C-terminal threonine residue (T198) enhances the binding to RhoA.[8] Cleavage of the C-terminal domain might alter the ability of p27 to bind and regulate RhoA. To test this hypothesis, we performed a co-immunoprecipitation analysis of full-length and truncated p27. As demonstrated previously,[63] RhoA co-immunoprecipitates with p27 (Figure 5a). In contrast, the truncated protein lacking the C-terminal 22 amino acids failed to interact with RhoA even under this condition of overexpression of both proteins (Figure 5a). This indicates that the C-terminal 22 amino acids of p27, which are removed by caspase processing, are required for stable interaction with the small GTPase RhoA. To determine whether truncation of p27 alters RhoA activation *in vivo*, we determined the abundance of active GTP-bound RhoA in pull-down assays. Whereas HeLa cells stably expressing full-length p27 had strongly reduced levels of active GTP-bound RhoA, cells expressing the truncated protein were characterized by a RhoA-GTP level similar to those of control cells (Figure 5b). The model that caspases render p27 unable to inhibit RhoA activation is supported by the observation that stress fiber formation can only be inhibited by overexpressing full-length p27 but not by overexpressing the truncated protein (Supplementary Figure 2).

Cleaved p27 fails to stimulate cell migration and invasion

One important physiological consequence of RhoA regulation by p27 is the induction of cell migration.[63] We speculated that truncated p27, which fails to bind RhoA, should no longer

stimulate cell migration. Using *in vitro* scratch assays,[64] we compared cell migration of p27-deficient MEFs reconstituted for expression of either full-length or truncated p27 to levels close to that of endogenous protein (Figure 4d). Following serum starvation cell migration was stimulated by the addition of fetal calf serum (Figures 5c and d) or PDGF (Supplementary Figure 3). As reported previously,[63] cells expressing full-length p27 exhibited increased cell motility. Importantly, the truncated protein was unable to stimulate cell migration (Figures 5c and d; Supplementary Figure 3). p27 has also been demonstrated to enhance cell invasion.[6–8] To investigate the effect of truncated p27 on cell invasion, we lentivirally transduced the invasive breast cancer cell line MDA-MB-231 with p27 mutants that do not inhibit CDK kinase activity (CK^-)[61] (Figure 5e). This should exclude

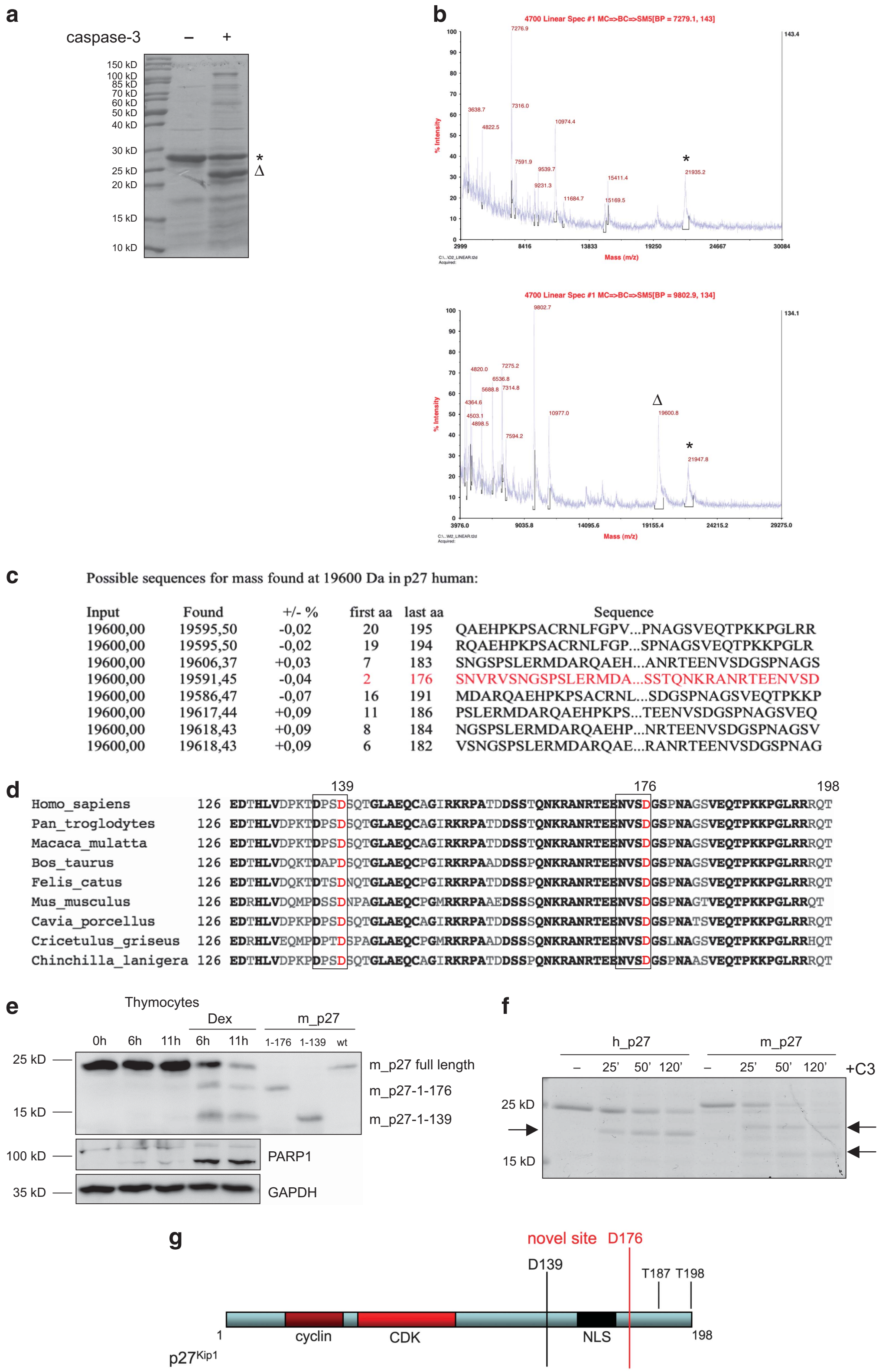
a
caspase-3 – +
150 kD
100 kD
85 kD
70 kD
60 kD
50 kD
40 kD
30 kD
25 kD
20 kD
15 kD
10 kD
b
4700 Linear Spec #1 MC=>BC=>SM5[BP = 7279.1, 143]
4700 Linear Spec #1 MC=>BC=>SM5[BP = 9802.9, 134]
% Intensity
Mass (m/z)
c
Possible sequences for mass found at 19600 Da in p27 human:
Input Found +/- % first aa last aa Sequence
19600,00 19595,50 -0,02 20 195 QAEHPKPSACRNLFGPV...PNAGSVEQTPKKPGLRR
19600,00 19595,50 -0,02 19 194 RQAEHPKPSACRNLFGP...SPNAGSVEQTPKKPGLR
19600,00 19606,37 +0,03 7 183 SNGSPSLERMDARQAEH...ANRTEENVSDGSPNAGS
19600,00 19591,45 -0,04 2 176 SNVRVSNGSPSLERMDA...SSTQNKRANRTEENVSD
19600,00 19586,47 -0,07 16 191 MDARQAEHPKPSACRNL...SDGSPNAGSVEQTPKKP
19600,00 19617,44 +0,09 11 186 PSLERMDARQAEHPKPS...TEENVSDGSPNAGSVEQ
19600,00 19618,43 +0,09 8 184 NGSPSLERMDARQAEHP...NRTEENVSDGSPNAGSV
19600,00 19618,43 +0,09 6 182 VSNGSPSLERMDARQAE...RANRTEENVSDGSPNAG
d
139 176 198
Homo_sapiens 126 EDTHLVDPKTDPSDSQTGLAEQCAGIRKRPATDDSSTQNKRANRTEENVSDGSPNAGSVEQTPKKPGLRRRQT
Pan_troglodytes 126 EDTHLVDPKTDPSDSQTGLAEQCAGIRKRPATDDSSTQNKRANRTEENVSDGSPNAGSVEQTPKKPGLRRRQT
Macaca_mulatta 126 EDTHLVDPKTDPSDSQTGLAEQCAGIRKRPATDDSSTQNKRANRTEENVSDGSPNAGSVEQTPKKPGLRRRQT
Bos_taurus 126 EDTHLVDQKTDAPDSQTGLAEQCPGIRKRPAADDSSPQNKRANRTEENVSDGSPNAGSVEQTPKKPGLRRRQT
Felis_catus 126 EDTHLVDQKTDTSDNQTGLAEQCPGIRKRPATDDSSPQNKRANRTEENVSDGSPNAGSVEQTPKKPGLRRRQT
Mus_musculus 126 EDRHLVDQMPDSSDNPAGLAEQCPGMRKRPAAEDSSSQNKRANRTEENVSDGSPNAGTVEQTPKKPGLRRQT
Cavia_porcellus 126 EDTHLVDPKPDPSDSQTGLAEQCAGIRKRPATDDSSSQNKRANRTEENVSDGSPNATSVEQTPKKPGLRRRQT
Cricetulus_griseus 126 EDRHLVEQMPDPTDSPAGLAEQCPGMRKRPAADDSSSQNKRANRTEENVSDGSLNAGSVEQTPKKPGLRRHQT
Chinchilla_lanigera 126 EDTHLVDPKPDPSDSQTGLAEQCAGIRKRPATDDSSPQNKRANRTEENVSDGSPNAASVEQTPKKPGLRRRQT
e
Thymocytes
Dex
m_p27
0h 6h 11h 6h 11h 1-176 1-139 wt
25 kD
15 kD
m_p27 full length
m_p27-1-176
m_p27-1-139
100 kD
PARP1
35 kD
GAPDH
f
h_p27
m_p27
– 25' 50' 120' – 25' 50' 120' +C3
25 kD
15 kD
g
novel site D176
D139
T187 T198
1
cyclin
CDK
NLS
198
p27Kip1

a potential contribution of different cell proliferation rates to the assay. The invasive capacities of cell lines expressing full-length or truncated p27 were compared in trans-well invasion assays. Expression of full-length p27 clearly enhanced invasion of stably transduced MDA-MB-231 cells (Figure 5f). This stimulatory effect was absent when the caspase cleavage product of p27 was expressed.

DISCUSSION

In this manuscript, we identify the caspase cleavage site of the human CDK inhibitor $p27^{Kip1}$. In contrast to previous speculations,[30,32,33] this site is located close to the C-terminus and does not separate the NLS from the CDK-inhibitory domain. Identification of this novel site is based on multiple lines of experimental evidence: Whereas mutation of the previously proposed site in the human protein fails to inhibit caspase processing, mutation at the novel cleavage site renders p27 resistant to caspase cleavage. The cleavage product is larger than the truncated p27 fragment 1–139 and co-migrates with a fragment of amino acids 1–176. Finally, mass spectrometry and N-terminal protein sequencing revealed that the product of p27 digestion with caspase-3 is a protein of amino acids 2–176. Of note, the region surrounding the newly identified cleavage motif is highly conserved among p27 orthologs from different mammalian species, contrasting the weaker conservation of the sequence surrounding D139. This suggests that caspase processing at D176 is conserved and an important mechanism of p27 regulation. The human protein carries a proline residue in position 137, which is predicted to disrupt the caspase processing site.[53,54] Interestingly, a number of mammalian species, including mice, express a p27 protein that maintains the second caspase consensus motif. Using primary mouse thymocytes, we can show that two fragments arise during apoptosis *in vivo*. Concurrently, using purified recombinant proteins and purified caspase, two fragments also originate from purified mouse p27, whereas the single larger fragment originates from the human protein. This suggests that the proline residue present in the human and other mammalian p27 may prevent cleavage. Importantly, the larger nuclear product is present following caspase activation in both species.

Compared with the closely related CDK inhibitor $p21^{Cip1/Waf1}$, caspase processing of human p27 does not separate the NLS from the CDK-inhibitory domain.[30] Consistently and in contrast to the smaller proposed product p23,[33] the novel identified caspase cleavage product of human p27 remains predominantly nuclear and binds and inhibits CDKs. This can explain earlier observations that p27 remains nuclear during apoptosis[30] and an inhibitor of CDK2.[29] In addition to maintaining the function of p27 as a potent inhibitor of CDK complexes, caspases can even lead to stabilization of the processed protein. Loss of domains recruiting ubiquitin ligases to p27 is one important consequence of the C-terminal truncation. These sequences include the C-terminal residue T198[1,58,65] and the phosphodegron surrounding T187. Upon phosphorylation of T187, p27 becomes a substrate of the ubiquitin ligase SCF-Skp2, which eventually leads to proteasomal degradation of p27.[1,38,66] Among the kinases that can phosphorylate T187 are active CDKs. Therefore, starting with CDK2 activation at the restriction point and until CDK inactivation in mitosis, a positive feedback loop leads to accelerated p27 degradation and increased CDK activation.[60] Processing by caspases can uncouple p27 from this feedback loop, leading to its stabilization in cell cycle phases where the protein is usually unstable. The robust stabilization of processed p27 may be especially important in caspase-induced differentiation,[17,18] where processing may contribute to a rigid accumulation of p27, and promote cell cycle arrest and cell cycle exit. Removal of the C-terminal phosphodegron resulting from caspase processing in differentiating cells could prevent unscheduled degradation, for example resulting from mitogen-induced T187 phosphorylation.[60]

When p27 is localized in the cytoplasm, a CDK-independent function is the regulation of cytoskeleton dynamics and cell motility. In fibrosarcoma cells, p27 was reported to inhibit cell motility by stoichiometrically interacting with the microtubule destabilizing protein stathmin (oncoprotein 18).[67] A second well-defined mechanism by which p27 contributes to the modulation of the cytoskeleton and cell motility is its ability to inhibit activation of the small GTPase, RhoA. Binding of p27 prevents RhoA association with guanine-nucleotide exchange factors and thereby the activation through GTP-binding.[4,63] This inhibition of RhoA activation reduces stress fiber formation, and promotes cell migration. The interaction with the small GTPase is mediated by the C-terminus of p27, and it was recently demonstrated that phosphorylation of the very C-terminus can regulate this interaction and that a p27 mutant 1–190 was unable to regulate RhoA.[8,68] Caspase processing of p27 abolishes this interaction and eliminates its ability to inhibit RhoA activation. During the execution of apoptosis cells undergo strong morphological changes that are partially controlled by the RhoA pathway.[69,70] p27 processing might contribute to increased RhoA activity like it is observed during apoptosis.

Reduction of cell motility after caspase processing of p27 may also be an important contribution to reduce spreading of pathogens, like viruses from infected cells during apoptosis. Limited cell invasion could help to keep cells within encapsulated areas and prevent cells to gain neighboring tissues.

p27 may further be especially important for non-lethal functions of caspases. It could for example be a means how caspases limit tumor progression without actually causing tumor cell death by reducing the invasive capacity of transformed cells. The CDK inhibitor is a crucial regulator of neurogenesis,[71–73] oligodendrocyte development[74] and the formation of the organ of corti.[42,75] Recently p27 was demonstrated to promote neuronal differentiation and cell migration in the cerebral cortex.[76] By modulating RhoA activity, p27 also

Figure 3. Identification of a novel and conserved caspase cleavage motif in p27 by mass spectrometry. **(a)** Recombinant purified p27 was incubated in presence + or absence − of a caspase-3 preparation. Proteins were separated by SDS–PAGE and stained with Coomassie brilliant blue. *, full-length p27; Δ, cleaved p27. (**b**) Analysis of the reaction in presence (bottom) or absence (top) of caspase-3 as shown in **a** by mass spectrometry (MALDI-TOF). The mass of peak fragments in Da is shown above the corresponding peaks. Upon caspase processing, the peak of 21.9 kDa declines and a novel peak of 19.6 kDa arises. *, peak for full-length p27; Δ, novel peak after incubation with caspase-3. (**c**) Table with p27 sequences that fit the mass of 19.6 kDa. A sequence starting at the N-terminus of the protein is highlighted in red. This sequence carries the aspartate residue 176 at the very C-terminus. (**d**) Alignment of the C-terminal sequences of p27 orthologs from different mammalian species. Caspase consensus sequences are shown in boxes. (**e**) Primary thymocytes were cultured with or without the addition of dexamethasone (10^{-7} M). Extracts from MEFs transiently overexpressing full-length and truncated forms of murine p27 were loaded for size comparison. The levels of transiently expressed p27 mutants were matched for western blot analysis. Extracts were blotted for p27, PARP1 and GAPDH. (**f**) Recombinant human and murine p27 were incubated with recombinant caspase-3 (C3). Samples were taken at the indicated time points (min). Proteins were separated by SDS–PAGE and stained with Coomassie brilliant blue. The caspase cleavage products are indicated by arrows. Human p27 was untagged and murine p27 carries an N-terminal 6xHis tag. −, purified p27 incubated in the absence of caspase-3. (**g**) Schematic representation of p27. The nuclear localization signal (NLS) and two C-terminal phosphorylation sites (T187 and T198) that can regulate p27 stability are indicated. A previously proposed and the newly identified caspase cleavage sites are shown.

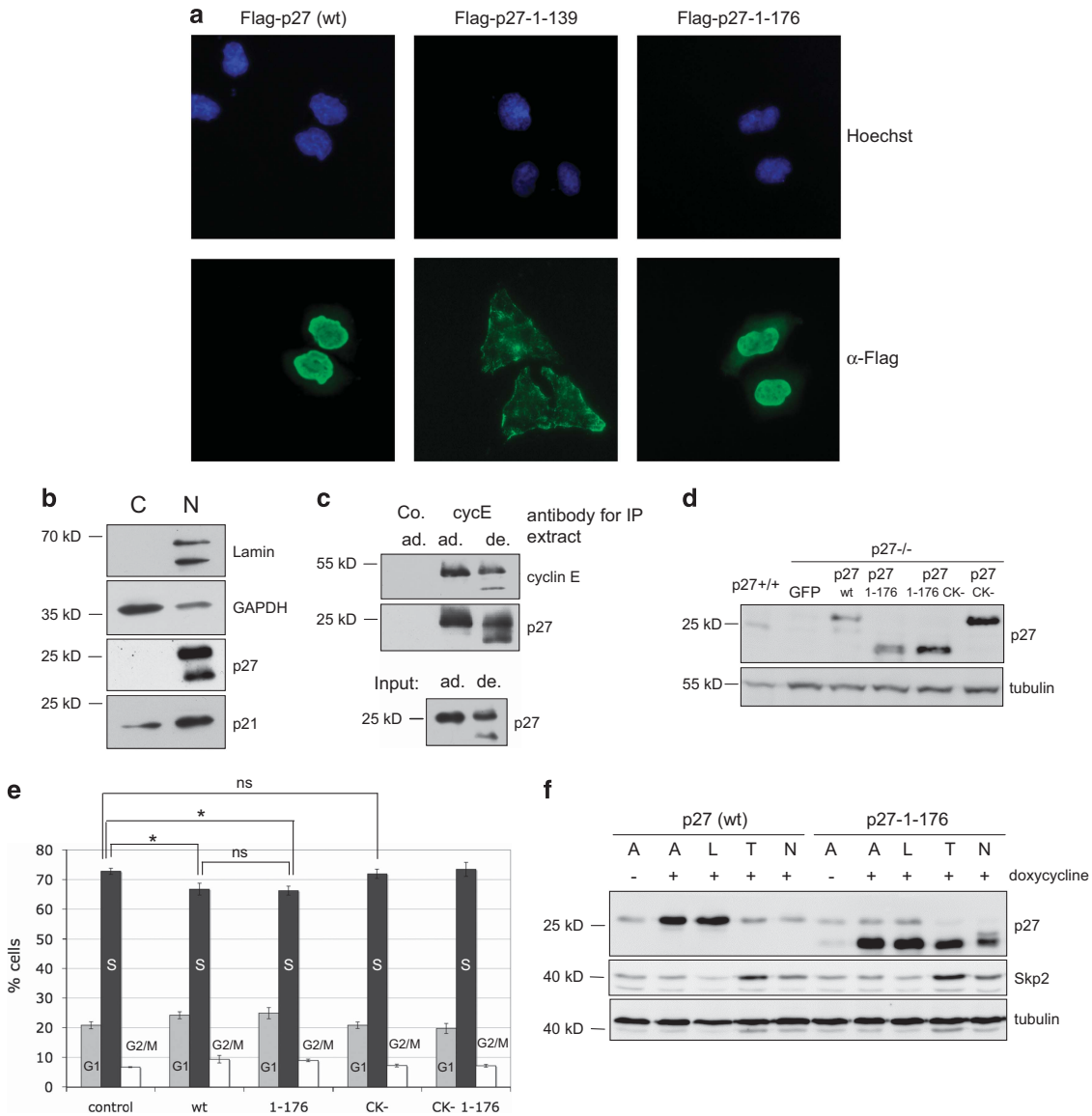

Figure 4. Caspase processed p27 remains nuclear and an inhibitor of cell cycle progression. (**a**) Immunofluorescence analysis of HeLa cells transfected with N-terminally Flag-tagged p27 proteins (wt, 1–139 and 1–176). The transfected proteins were detected with anti-Flag antibodies and marked with Alexa Fluor 488 labeled secondary antibodies (bottom panel, green). The DNA was stained with Hoechst (top panel, blue). Representative pictures from three independent biological experiments are shown. (**b**) Subcellular fractionation of apoptotic WM35 melanoma cells and subsequent analysis of endogenous p21, p27, lamin and GAPDH in cytosolic (C) and nuclear (N) fractions. GAPDH and lamin served as controls for the cytoplasmic or nuclear fractions. Representative blots of three independent experiments are shown. (**c**) Cyclin E binds to caspase processed p27 in apoptotic cells. WM35 melanoma-derived cells were irradiated with UV (80 J/m^2) and cyclin E complexes were immunoprecipitated. Immunoprecipitates of endogenous proteins were analyzed for cyclin E and co-immunoprecipitated p27. ad. indicates adherent cells; de. indicates detached (apoptotic) cells; Co. indicates control immunoprecipitation with anti-HA antibodies. **(d)** p27 knockout MEFs (p27$^{-/-}$) were lentivirally transduced with p27 mutants as indicated. Protein extracts were blotted for p27 and β-tubulin. (**e**) Moderate expression of p27 or p27-1–176 both lead to a moderate increase in G1 and a moderate decline in S-phase cells. Bar graph representing cell cycle analysis of p27 knockout MEFs constitutively expressing the indicated variants of p27 or a GFP-vector (control). G1 (% of cells in G1 phase); S (% of cells in S phase); G2/M (% of cells in G2 or M phase). Graph represents the mean values of three independent biological experiments with standard deviations. *$P < 0.01$ by Student's *t*-test of percentage of cells in S phase; NS, non significant difference in S phase percentage by Student's *t*-test. (**f**) HeLa T-REx Flp-In cells inducibly expressing either p27 wild-type (wt) or p27-1–176 were grown asynchronously (A) or arrested with either lovastatin (L), thymidine (T) or nocodazole (N) for 16 h. Subsequently, p27 protein expression was induced with doxycycline (1 μM) for 8 h. Total cell extracts were blotted for p27, Skp2 and β-tubulin. Lovastatin was added at a final concentration of 40 μM. Thymidine was added at a final concentration of 2 mM. Nocodazole was added at a final concentration of 50 ng/ml. Representative blots of three independent experiments are shown.

regulates the morphological remodeling and the motility of neurons.[68] As caspases fulfil non-lethal roles in neuron cell differentiation,[28,73,77] processing of p27 during neuronal development could be an important regulatory mechanism to mediate a robust cell cycle exit as well as trigger cytoskeletal remodeling. Similarly, the expression of p27 is associated with cell cycle arrest and differentiation in hematopoietic cells[40,41,43] where it is crucial for the maintenance of stem cell quiescence.[78] Interestingly, caspase-3 has recently been revealed to be a regulator of hematopoietic stem cell quiescence.[79]

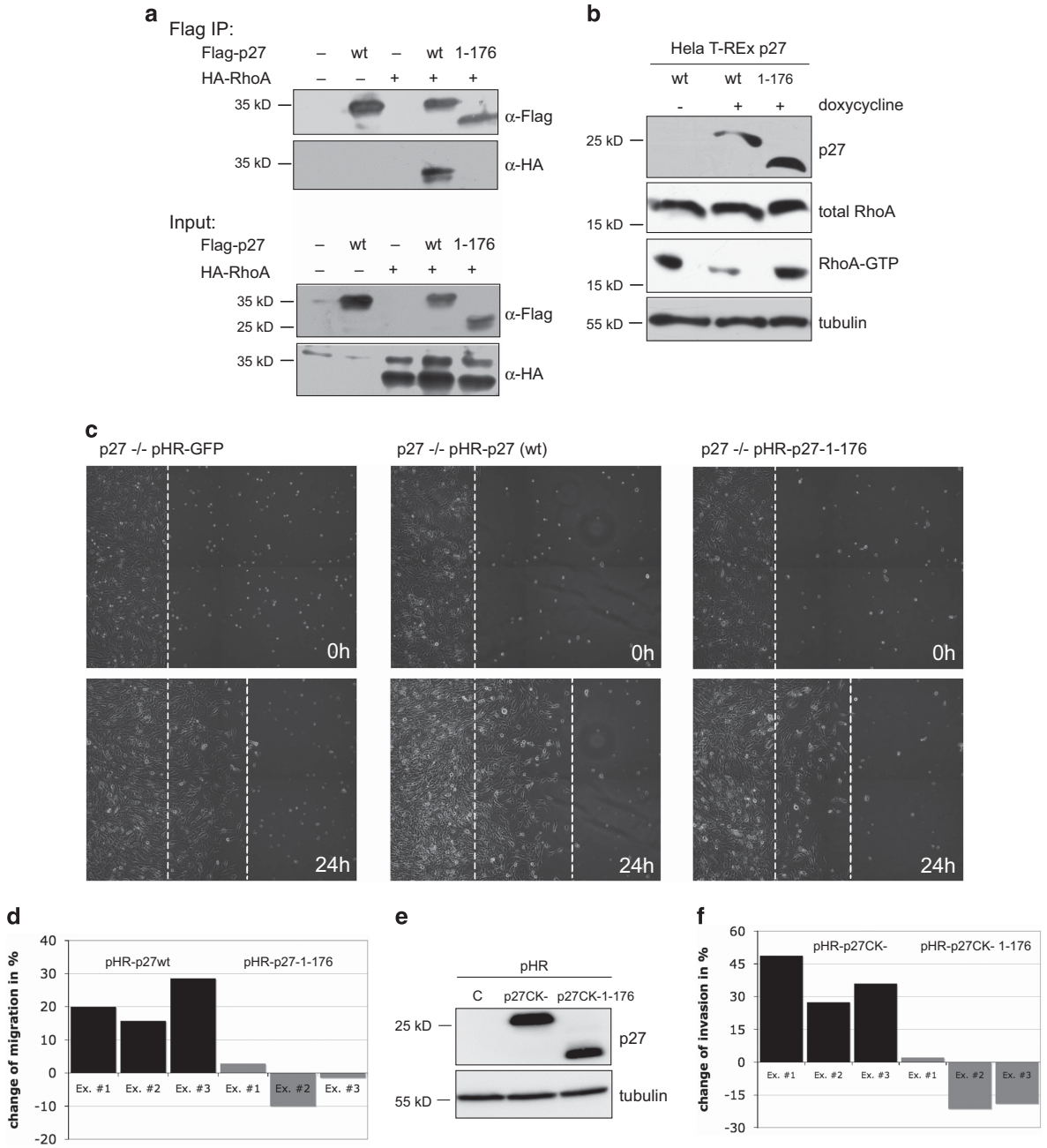

Figure 5. Caspase processing of p27 abolishes RhoA binding and inhibition, and p27 dependent induction of cell migration and cell invasion. (**a**) Flag-tagged p27 proteins (wt or 1–176) were co-expressed with HA-tagged RhoA in HeLa cells. The immunoprecipitation of Flag-tagged proteins was subjected to western blot analysis for Flag- and potentially co-immunoprecipitated HA-tagged proteins (FLAG-IP, upper panels). The abundance of expressed proteins in total extracts is shown in western blot analysis (Input, lower panels). A representative experiment of three independent biological experiments is shown. (**b**) Pull-down assay for active GTP-bound RhoA from HeLa T-REx cells stably expressing p27 wild-type or a mutant p27 truncated at residue 176. The input and the pull-down fractions were blotted for p27, RhoA and β-tubulin. A representative blot of three independent biological experiments is shown. (**c**) Migration analysis of lentivirally transfected MEFs (GFP, p27 wt, p27-1-176) by time-lapse video microscopy. Pictures taken at 0 and 24 h are shown. Cells were serum starved for 36 h (0.1% FCS). At 0 h, cells were stimulated with 10% FCS and scratches performed as described in the methods. The border of adherent cells is marked by the dotted line. After 24 h, migration into the gap was determined and the novel border was indicated with a second dashed line (lower panels, right lines). The distance of cell migration by adherent cells was determined and compared to a GFP-transfected control. One out of three independent biological experiments summarized in (d, Exeriment #2) is shown. (**d**) Comparison of cell migration of p27 wt and p27-1–176 in comparison to GFP-transfected control cells. The relative increase or decrease compared to GFP-transfected cells is shown in percent. Three independent experiments (Ex.#1, Ex#2, Ex#3) as in **c** are shown. (**e**) MDA-MB-231 breast cancer cells were lentivirally transduced with a control plasmid (C), p27CK^{-} or p27CK^{-}-1-176. Extracts were blotted for p27 and β-tubulin. 'C' indicates MDA-MB-231 cells transduced with a p27 construct in which codon 2 was mutated to a stop codon, which results in no exogenous expression of p27. (**f**) Transduced MDA-MB-231 cells were analyzed in transwell cell invasion assays and analyzed for cell invasion after 20 h. The changes of invasion in percent compared to cells transduced with a control plasmid are shown.

In addition to their key role in programmed cell death, caspases exert non-lethal functions in diverse processes including inflammation, cell differentiation or tissue remodeling. We have now identified the caspase cleavage site in human p27 and observed that caspase processing does neither alter localization nor CDK inhibition of human p27. Removal of a C-terminal phosphodegron stabilizes p27 by uncoupling its stability from cell cycle regulated proteolysis. In addition, caspase cleavage abolishes the ability of p27 to stimulate cell migration and cell invasion. By inducing a robust CDK inhibition combined with regulation of cytoskeletal remodelling, processing of p27 could promote non-lethal functions of caspases for example in cell cycle exit and differentiation. It will be exciting to determine the contribution of caspase cleavage of p27 in these processes in the future, for example, by knock-in of a caspase resistant p27 allele.

MATERIALS AND METHODS

Cell culture and treatments

WM35 (laboratory of Joyce Slingerland) and CCRF-CEM-C7H2 (CEM) (laboratory of Reinhard Kofler) cells were grown in RPMI (Sigma-Aldrich, St. Louis, MO, USA), 10% fetal calf serum (FCS; PAA, Pasching, Upper Austria, Austria), penicillin/streptomycin (Sigma-Aldrich). HeLa, HeLa T-REx (Invitrogen, Carlsbad, CA, USA), MDA-MB-231 (laboratory of Stephan Geley) and MEFs (laboratory of Nisar Malek) were cultured in Dulbecco's modified Eagle media (Sigma-Aldrich), 10% FCS (PAA), penicillin/streptomycin. Cells were irradiated in a UV Stratalinker 1800 (Stratagene, La Jolla, CA, USA). Cells were lyzed in Laemmli buffer[80] or IP-buffer[81] using an ultrasonic homogenizer (Sonoplus, Bandelin, Berlin, Germany). Subcellular fractionation was performed as previously described.[31] Thymocytes were isolated from the thymus of a 4-week-old male C57BL/6 mouse using a sterile cell strainer (#352360, BD, Heidelberg, Germany). Single cells were grown in RPMI (Sigma-Aldrich), 10% FCS (PAA), 50 μM β-mercaptoethanol (Sigma-Aldrich), 1 mM pyruvate (Gibco Life Technologies, Carlsbad, CA, USA), penicillin/streptomycin (Sigma-Aldrich) with or without dexamethasone (10^{-7} M).

Antibodies and reagents

anti-p27 (mouse monoclonal anti-p27 #610242, BD Transduction Laboratories, Franklin Lakes, NJ, USA), anti-p21 (mouse monoclonal anti-human Cip1 #610234, BD), anti-Skp2 (rabbit polyclonal sc-7164, Santa Cruz, Santa Cruz, CA, USA), anti-β-tubulin (mouse monoclonal β-tubulin AA2 #T8328, Sigma-Aldrich), anti-active-caspase-3 (rabbit monoclonal 5A1E #9664, Cell Signaling, Danvers, MA, USA), anti-cyclin D1 (mouse monoclonal DCS6 sc-20044, Santa Cruz), anti-cyclin E (mouse monoclonal HE12 sc-247, Santa Cruz), anti-cyclin E (mouse monoclonal HE172 #32–1500, Invitrogen), anti-cyclin A (polyclonal rabbit serum, Hengst laboratory), anti-cyclin B1 (mouse monoclonal #V152, Cell Signaling), anti-RhoA (rabbit monoclonal #2117 (67B9), Cell Signaling), anti-PARP (rabbit monoclonal 46D11 #9532, Cell Signaling), anti-lamin A/C (mouse monoclonal clone14, Upstate, Millipore, Billerica, MA, USA), anti-GAPDH (mouse monoclonal 6C5 ab8245, Abcam), anti-Flag (mouse monoclonal M2 #F3165, Sigma-Aldrich), anti-HA (mouse monoclonal 12CA5 ab16918, Abcam, Cambridge, MA, USA), horse raddish peroxidase-conjugated anti–His antibody (His-probe sc-8083, Santa Cruz).

Dexamethasone (D4902, Sigma-Aldrich), digitonin (D5628, Sigma-Aldrich), propidium iodide (PI) (81845, Sigma-Aldrich), doxycycline (#44577, Sigma-Aldrich), lovastatin (#L-154, MERCK, Darmstadt, Germany), thymidine (#T9250, Sigma-Aldrich), nocodazole (#1404, Sigma-Aldrich) and PDGF (PeproTech, Rocky Hill, NJ, USA).

Plasmids

For cloning the Gateway recombination cloning system (Invitrogen) was used. p27 mutants were generated by site-directed mutagenesis. In BP reactions (Invitrogen) PCR products were recombined with the pDONR207 (Invitrogen) vector. Entry vectors were recombined with destination vectors carrying the desired tags (LR reactions, Invitrogen). To generate stable cell lines, pTO destination vectors (generated by Stephan Geley) were co-transfected with the Flp-recombinase expression vector pOG44 (Invitrogen). To lentivirally transduce $p27^{-/-}$ MEFs and MDA-MB-231 cells, the plasmids pHR-SFFV-IR-puroSG (a generous gift from Stephan Geley), pVSVG-G (Invitrogen) and psPAX2 (Addgene, Cambridge, MA, USA) were used. pET3c-p27 (wild-type) was used to produce recombinant untagged human p27. Murine p27 was cloned into pET21eSG (a generous gift from Stephan Geley) for expression in *E. coli*. Rho binding domain of rhotekin was expressed in *E. coli* using pGEX-2 T-RBD. For transfection Lipofectamine 2000 (Invitrogen) or PolyFect (Qiagen, Venlo, Netherlands) were used.

Recombinant proteins and *in vitro* cleavage assays

Recombinant p27 mutants and caspases were expressed in *E. coli* BL21 (DE3). His-tagged proteins were purified by Ni^{2+}-affinity chromatography (Invitrogen).

Caspase cleavage reactions were set up in 10 mM HEPES pH7, 300 mM sucrose, 10 mM KCl, 10 mM DTT, 1.5 mM $MgCl_2$, 0.5% NP40, plus protease inhibitors (SIGMA*FAST*, Sigma-Aldrich) for caspases 3, 7 and 8; in 25 mM HEPES pH7, 300 mM sucrose, 10 mM KCl, 10 mM DTT, 1,5 mM $MgCl_2$, plus protease inhibitors (SIGMA*FAST*™, Sigma-Aldrich) for caspase-2.

Immunoblotting, immunoprecipitation and pull-down assays

Proteins were transferred to PVDF membranes (Immobilon IPVH00010, Millipore) by electroblotting. Primary antibodies were detected using horse raddish peroxidase-coupled secondary antibodies and chemiluminescence. For immunoprecipitation, total cell lysates were incubated with antibodies and protein A (Immunosorb A 10–1257, Medicago, Durham, NC, USA) or protein G (Fast Flow 16–266, Millipore) agarose beads. To pull-down active RhoA, cell lysates were incubated with GST-tagged Rhotekin Rho-binding domain and glutathione sepharose beads (Sepharose 4B, GE Healthcare Life Sciences, Little Chalfont, UK).

Microscopy and migration experiments

Paraformaldehyde-fixed cells were incubated with mouse anti-Flag antibodies, and stained with anti-mouse Alexa Fluor488 antibodies (Invitrogen) and Hoechst 33342 (Sigma-Aldrich). A Zeiss M2 microscope (Zeiss, Jena, Germany) and MetaMorph software (Molecular Devices, Sunnyvale, CA, USA) were used.

Scratch assays were analyzed with a Cell-IQ (CM-Tech, Tampere, Finland) cell imaging platform. To produce defined cell-free gaps, cell culture inserts (#80241, Ibidi, Martinsried, Germany) were used.

Cell Invasion experiments

Cells were seeded in the apical chambers of Corning BioCoat Tumor Invasion System Fluoroblok24-well plates (5×10^5 cells), labelled with DilC12(3) Fluorescent Dye (BD) and incubated in an Infinite F200 plate reader (Tecan, Männerdorf, Switzerland) at 37 °C. Experiments were carried out according to the instructions of the supplier. For each condition cells were seeded in triplicate.

FACS cell cycle analysis

A standard protocol for bromodeoxyuridine (BrdU) and propidium iodide (PI) staining was used. For FACS a Becton Dickinson flow cytometer (BD) was used and profiles were analyzed with the FlowJo (Tree Star, Ashland, OR, USA) software. Transfected (GFP-positve) 293 T cells were analyzed basically following the method described in Kalejta *et al.*[82]

Mass spectrometry and N-terminal sequencing

Mass spectrometry analysis was performed on a MALDI TOF/TOF 4800 Plus Analyzer (ABSCIEX, Framingham, MA, USA). For N-terminal sequencing the ABI Procise Model 492 Edman Micro Sequencer connected to an ABI Model 140C PTH Amino Acid Analyzer was used.

Sequence alignment

Protein sequences were aligned using the STRAP alignment program (Institut für Biochemie, Charité, Berlin).

CONFLICT OF INTEREST

The authors declare no conflict of interest.

ACKNOWLEDGEMENTS

We acknowledge Stephan Geley for providing plasmids and cell lines, Jan Wiegers for useful advice with mouse experiments and all members of the Hengst lab for their help and stimulating discussions. Work was funded by the FWF-grant P24031 to Ludger Hengst, the FWF-grant P26856 to Andreas Villunger and the Tiroler Krebshilfe.

REFERENCES

1 Chu IM, Hengst L, Slingerland JM. The Cdk inhibitor p27 in human cancer: prognostic potential and relevance to anticancer therapy. *Nat Rev Cancer* 2008; **8**: 253–267.
2 Sherr CJ, Roberts JM. CDK inhibitors: positive and negative regulators of G1-phase progression. *Genes Dev* 1999; **13**: 1501–1512.
3 Lacy ER, Filippov I, Lewis WS, Otieno S, Xiao L, Weiss S *et al.* p27 binds cyclin-CDK complexes through a sequential mechanism involving binding-induced protein folding. *Nat Struct Mol Biol* 2004; **11**: 358–364.
4 Besson A, Dowdy SF, Roberts JM. CDK inhibitors: cell cycle regulators and beyond. *Dev Cell* 2008; **14**: 159–169.
5 Besson A, Hwang HC, Cicero S, Donovan SL, Gurian-West M, Johnson D *et al.* Discovery of an oncogenic activity in p27Kip1 that causes stem cell expansion and a multiple tumor phenotype. *Genes Dev* 2007; **21**: 1731–1746.
6 Zhao D, Besser AH, Wander SA, Sun J, Zhou W, Wang B *et al.* Cytoplasmic p27 promotes epithelial-mesenchymal transition and tumor metastasis via STAT3-mediated Twist1 upregulation. *Oncogene* 2015; **34**: 5447–5459.
7 See WL, Heinberg AR, Holland EC, Resh MD. p27 deficiency is associated with migration defects in PDGF-expressing gliomas in vivo. *Cell Cycle* 2010; **9**: 1562–1567.
8 Larrea MD, Hong F, Wander SA, da Silva TG, Helfman D, Lannigan D *et al.* RSK1 drives p27Kip1 phosphorylation at T198 to promote RhoA inhibition and increase cell motility. *Proc Natl Acad Sci USA* 2009; **106**: 9268–9273.
9 Slingerland JM, Hengst L, Pan CH, Alexander D, Stampfer MR, Reed SI. A novel inhibitor of cyclin-Cdk activity detected in transforming growth factor beta-arrested epithelial cells. *Mol Cell Biol* 1994; **14**: 3683–3694.
10 Polyak K, Kato JY, Solomon MJ, Sherr CJ, Massague J, Roberts JM *et al.* p27Kip1, a cyclin-Cdk inhibitor, links transforming growth factor-beta and contact inhibition to cell cycle arrest. *Genes Dev* 1994; **8**: 9–22.
11 Hengst L, Dulic V, Slingerland JM, Lees E, Reed SI. A cell cycle-regulated inhibitor of cyclin-dependent kinases. *Proc Natl Acad Sci USA* 1994; **91**: 5291–5295.
12 Toyoshima H, Hunter T. p27, a novel inhibitor of G1 cyclin-Cdk protein kinase activity, is related to p21. *Cell* 1994; **78**: 67–74.
13 Polyak K, Lee MH, Erdjument-Bromage H, Koff A, Roberts JM, Tempst P *et al.* Cloning of p27Kip1, a cyclin-dependent kinase inhibitor and a potential mediator of extracellular antimitogenic signals. *Cell* 1994; **78**: 59–66.
14 Katayose Y, Kim M, Rakkar AN, Li Z, Cowan KH, Seth P. Promoting apoptosis: a novel activity associated with the cyclin-dependent kinase inhibitor p27. *Cancer Res* 1997; **57**: 5441–5445.
15 Hiromura K, Pippin JW, Fero ML, Roberts JM, Shankland SJ. Modulation of apoptosis by the cyclin-dependent kinase inhibitor p27(Kip1). *J Clin Invest* 1999; **103**: 597–604.
16 Taylor RC, Cullen SP, Martin SJ. Apoptosis: controlled demolition at the cellular level. *Nat Rev Mol Cell Biol* 2008; **9**: 231–241.
17 Fuchs Y, Steller H. Programmed cell death in animal development and disease. *Cell* 2011; **147**: 742–758.
18 Lamkanfi M, Festjens N, Declercq W, Vanden Berghe T, Vandenabeele P. Caspases in cell survival, proliferation and differentiation. *Cell Death Differ* 2007; **14**: 44–55.
19 Ashkenazi A, Salvesen G. Regulated cell death: signaling and mechanisms. *Annu Rev Cell Dev Biol* 2014; **30**: 337–356.
20 Cotter TG. Apoptosis and cancer: the genesis of a research field. *Nat Rev Cancer* 2009; **9**: 501–507.
21 Eymin B, Haugg M, Droin N, Sordet O, Dimanche-Boitrel MT, Solary E. p27Kip1 induces drug resistance by preventing apoptosis upstream of cytochrome c release and procaspase-3 activation in leukemic cells. *Oncogene* 1999; **18**: 1411–1418.
22 Bryja V, Pachernik J, Soucek K, Horvath V, Dvorak P, Hampl A. Increased apoptosis in differentiating p27-deficient mouse embryonic stem cells. *Cell Mol Life Sci* 2004; **61**: 1384–1400.
23 Liang J, Shao SH, Xu ZX, Hennessy B, Ding Z, Larrea M *et al.* The energy sensing LKB1-AMPK pathway regulates p27(kip1) phosphorylation mediating the decision to enter autophagy or apoptosis. *Nat Cell Biol* 2007; **9**: 218–224.
24 Fan XM, Tu SP, Lam SK, Wang WP, Wu J, Wong WM *et al.* Five-lipoxygenase-activating protein inhibitor MK-886 induces apoptosis in gastric cancer through upregulation of p27kip1 and bax. *J Gastroenterol Hepatol* 2004; **19**: 31–37.
25 Zhang R, Banik NL, Ray SK. Combination of all-trans retinoic acid and interferon-gamma upregulated p27(kip1) and down regulated CDK2 to cause cell cycle arrest leading to differentiation and apoptosis in human glioblastoma LN18 (PTEN-proficient) and U87MG (PTEN-deficient) cells. *Cancer Chemother Pharmacol* 2008; **62**: 407–416.
26 Woltman AM, van der Kooij SW, Coffer PJ, Offringa R, Daha MR, van Kooten C. Rapamycin specifically interferes with GM-CSF signaling in human dendritic cells, leading to apoptosis via increased p27KIP1 expression. *Blood* 2003; **101**: 1439–1445.
27 Riedl SJ, Shi Y. Molecular mechanisms of caspase regulation during apoptosis. *Nat Rev Mol Cell Biol* 2004; **5**: 897–907.
28 Shalini S, Dorstyn L, Dawar S, Kumar S. Old new and emerging functions of caspases. *Cell Death Differ* 2014; **22**: 526–539.
29 Eymin B, Sordet O, Droin N, Munsch B, Haugg M, Van de Craen M *et al.* Caspase-induced proteolysis of the cyclin-dependent kinase inhibitor p27Kip1 mediates its anti-apoptotic activity. *Oncogene* 1999; **18**: 4839–4847.
30 Levkau B, Koyama H, Raines EW, Clurman BE, Herren B, Orth K *et al.* Cleavage of p21Cip1/Waf1 and p27Kip1 mediates apoptosis in endothelial cells through activation of Cdk2: role of a caspase cascade. *Mol Cell* 1998; **1**: 553–563.
31 Connor MK, Kotchetkov R, Cariou S, Resch A, Lupetti R, Beniston RG *et al.* CRM1/Ran-mediated nuclear export of p27(Kip1) involves a nuclear export signal and links p27 export and proteolysis. *Mol Biol Cell* 2003; **14**: 201–213.
32 Kurokawa M, Kornbluth S. Caspases and kinases in a death grip. *Cell* 2009; **138**: 838–854.
33 Loubat A, Rochet N, Turchi L, Rezzonico R, Far DF, Auberger P *et al.* Evidence for a p23 caspase-cleaved form of p27[KIP1] involved in G1 growth arrest. *Oncogene* 1999; **18**: 3324–3333.
34 Harvey KJ, Lukovic D, Ucker DS. Caspase-dependent Cdk activity is a requisite effector of apoptotic death events. *J Cell Biol* 2000; **148**: 59–72.
35 Kumar S. Caspase function in programmed cell death. *Cell Death Differ* 2007; **14**: 32–43.
36 Guicciardi ME, Gores GJ. Life and death by death receptors. *Faseb J* 2009; **23**: 1625–1637.
37 Starostina NG, Kipreos ET. Multiple degradation pathways regulate versatile CIP/KIP CDK inhibitors. *Trends Cell Biol* 2011; **22**: 33–41.
38 Nakayama KI, Nakayama K. Ubiquitin ligases: cell-cycle control and cancer. *Nat Rev Cancer* 2006; **6**: 369–381.
39 Nguyen L, Besson A, Roberts JM, Guillemot F. Coupling cell cycle exit, neuronal differentiation and migration in cortical neurogenesis. *Cell Cycle* 2006; **5**: 2314–2318.
40 Yaroslavskiy B, Watkins S, Donnenberg AD, Patton TJ, Steinman RA. Subcellular and cell-cycle expression profiles of CDK-inhibitors in normal differentiating myeloid cells. *Blood* 1999; **93**: 2907–2917.
41 Taniguchi T, Endo H, Chikatsu N, Uchimaru K, Asano S, Fujita T *et al.* Expression of p21(Cip1/Waf1/Sdi1) and p27(Kip1) cyclin-dependent kinase inhibitors during human hematopoiesis. *Blood* 1999; **93**: 4167–4178.
42 Chen P, Segil N. p27(Kip1) links cell proliferation to morphogenesis in the developing organ of Corti. *Development* 1999; **126**: 1581–1590.
43 Rots NY, Iavarone A, Bromleigh V, Freedman LP. Induced differentiation of U937 cells by 1,25-dihydroxyvitamin D3 involves cell cycle arrest in G1 that is preceded by a transient proliferative burst and an increase in cyclin expression. *Blood* 1999; **93**: 2721–2729.
44 Matsuoka S, Ballif BA, Smogorzewska A, McDonald ER 3rd, Hurov KE, Luo J *et al.* ATM and ATR substrate analysis reveals extensive protein networks responsive to DNA damage. *Science* 2007; **316**: 1160–1166.
45 Dix MM, Simon GM, Wang C, Okerberg E, Patricelli MP, Cravatt BF. Functional interplay between caspase cleavage and phosphorylation sculpts the apoptotic proteome. *Cell* 2012; **150**: 426–440.
46 Tozser J, Bagossi P, Zahuczky G, Specht SI, Majerova E, Copeland TD. Effect of caspase cleavage-site phosphorylation on proteolysis. *Biochem J* 2003; **372**: 137–143.
47 Stennicke HR, Renatus M, Meldal M, Salvesen GS. Internally quenched fluorescent peptide substrates disclose the subsite preferences of human caspases 1, 3, 6, 7 and 8. *Biochem J* 2000; **350**: 563–568.
48 Tambyrajah WS, Bowler LD, Medina-Palazon C, Sinclair AJ. Cell cycle-dependent caspase-like activity that cleaves p27(KIP1) is the beta(1) subunit of the 20S proteasome. *Arch Biochem Biophys* 2007; **466**: 186–193.
49 Medina-Palazon C, Bernard E, Frost V, Morley S, Sinclair AJ. KIPase activity is a novel caspase-like activity associated with cell proliferation. *Eur J Biochem* 2004; **271**: 2716–2723.
50 Mazumder S, Gong B, Chen Q, Drazba JA, Buchsbaum JC, Almasan A. Proteolytic cleavage of cyclin E leads to inactivation of associated kinase activity and amplification of apoptosis in hematopoietic cells. *Mol Cell Biol* 2002; **22**: 2398–2409.
51 Schmidt S, Rainer J, Ploner C, Presul E, Riml S, Kofler R. Glucocorticoid-induced apoptosis and glucocorticoid resistance: molecular mechanisms and clinical relevance. *Cell Death Differ* 2004; **11**: S45–S55.
52 Kullmann MK, Grubbauer C, Goetsch K, Jakel H, Podmirseg SR, Trockenbacher A *et al.* The p27-Skp2 axis mediates glucocorticoid-induced cell cycle arrest in T-lymphoma cells. *Cell Cycle* 2013; **12**: 2625–2635.
53 Crawford ED, Seaman JE, Agard N, Hsu GW, Julien O, Mahrus S *et al.* The DegraBase: a database of proteolysis in healthy and apoptotic human cells. *Mol Cell Proteomics* 2013; **12**: 813–824.

54 Thornberry NA, Rano TA, Peterson EP, Rasper DM, Timkey T, Garcia-Calvo M *et al.* A combinatorial approach defines specificities of members of the caspase family and granzyme B. Functional relationships established for key mediators of apoptosis. *J Biol Chem* 1997; **272**: 17907–17911.
55 Werlen G, Hausmann B, Naeher D, Palmer E. Signaling life and death in the thymus: timing is everything. *Science* 2003; **299**: 1859–1863.
56 Perandones CE, Illera VA, Peckham D, Stunz LL, Ashman RF. Regulation of apoptosis in vitro in mature murine spleen T cells. *J Immunol* 1993; **151**: 3521–3529.
57 Vervoorts J, Luscher B. Post-translational regulation of the tumor suppressor p27 (KIP1). *Cell Mol Life Sci* 2008; **65**: 3255–3264.
58 Kossatz U, Vervoorts J, Nickeleit I, Sundberg HA, Arthur JS, Manns MP *et al.* C-terminal phosphorylation controls the stability and function of p27kip1. *EMBO J* 2006; **25**: 5159–5170.
59 Schiappacassi M, Lovisa S, Lovat F, Fabris L, Colombatti A, Belletti B *et al.* Role of T198 modification in the regulation of p27(Kip1) protein stability and function. *PLoS ONE* 2011; **6**: e17673.
60 Jakel H, Peschel I, Kunze C, Weinl C, Hengst L. Regulation of p27 (Kip1) by mitogen-induced tyrosine phosphorylation. *Cell Cycle* 2012; **11**: 1910–1917.
61 Vlach J, Hennecke S, Amati B. Phosphorylation-dependent degradation of the cyclin-dependent kinase inhibitor p27. *EMBO J* 1997; **16**: 5334–5344.
62 Vosper J, Masuccio A, Kullmann M, Ploner C, Geley S, Hengst L. Statin-induced depletion of geranylgeranyl pyrophosphate inhibits cell proliferation by a novel pathway of Skp2 degradation. *Oncotarget* 2014; **6**: 2889–2902.
63 Besson A, Gurian-West M, Schmidt A, Hall A, Roberts JM. p27Kip1 modulates cell migration through the regulation of RhoA activation. *Genes Dev* 2004; **18**: 862–876.
64 Liang CC, Park AY, Guan JL. In vitro scratch assay: a convenient and inexpensive method for analysis of cell migration in vitro. *Nat Protoc* 2007; **2**: 329–333.
65 De Vita F, Riccardi M, Malanga D, Scrima M, De Marco C, Viglietto G. PKC-dependent phosphorylation of p27 at T198 contributes to p27 stabilization and cell cycle arrest. *Cell Cycle* 2012; **11**: 1583–1592.
66 Bloom J, Pagano M. Deregulated degradation of the cdk inhibitor p27 and malignant transformation. *Semin Cancer Biol* 2003; **13**: 41–47.
67 Baldassarre G, Belletti B, Nicoloso MS, Schiappacassi M, Vecchione A, Spessotto P *et al.* p27(Kip1)-stathmin interaction influences sarcoma cell migration and invasion. *Cancer Cell* 2005; **7**: 51–63.
68 Godin JD, Thomas N, Laguesse S, Malinouskaya L, Close P, Malaise O *et al.* p27(Kip1) is a microtubule-associated protein that promotes microtubule polymerization during neuron migration. *Dev Cell* 2012; **23**: 729–744.
69 Croft DR, Coleman ML, Li S, Robertson D, Sullivan T, Stewart CL *et al.* Actin-myosin-based contraction is responsible for apoptotic nuclear disintegration. *J Cell Biol* 2005; **168**: 245–255.
70 Coleman ML, Olson MF. Rho GTPase signalling pathways in the morphological changes associated with apoptosis. *Cell Death Differ* 2002; **9**: 493–504.
71 Cremisi F, Philpott A, Ohnuma S. Cell cycle and cell fate interactions in neural development. *Curr Opin Neurobiol* 2003; **13**: 26–33.
72 Doetsch F, Verdugo JM, Caille I, Alvarez-Buylla A, Chao MV, Casaccia-Bonnefil P. Lack of the cell-cycle inhibitor p27Kip1 results in selective increase of transit-amplifying cells for adult neurogenesis. *J Neurosci* 2002; **22**: 2255–2264.
73 Dehay C, Kennedy H. Cell-cycle control and cortical development. *Nat Rev Neurosci* 2007; **8**: 438–450.
74 Durand B, Raff M. A cell-intrinsic timer that operates during oligodendrocyte development. *Bioessays* 2000; **22**: 64–71.
75 Lowenheim H, Furness DN, Kil J, Zinn C, Gultig K, Fero ML *et al.* Gene disruption of p27(Kip1) allows cell proliferation in the postnatal and adult organ of corti. *Proc Natl Acad Sci USA* 1999; **96**: 4084–4088.
76 Nguyen L, Besson A, Heng JI, Schuurmans C, Teboul L, Parras C *et al.* p27kip1 independently promotes neuronal differentiation and migration in the cerebral cortex. *Genes Dev* 2006; **20**: 1511–1524.
77 Hyman BT, Yuan J. Apoptotic and non-apoptotic roles of caspases in neuronal physiology and pathophysiology. *Nat Rev Neurosci* 2012; **13**: 395–406.
78 Zou P, Yoshihara H, Hosokawa K, Tai I, Shinmyozu K, Tsukahara F *et al.* p57(Kip2) and p27(Kip1) cooperate to maintain hematopoietic stem cell quiescence through interactions with Hsc70. *Cell Stem Cell* 2011; **9**: 247–261.
79 Janzen V, Fleming HE, Riedt T, Karlsson G, Riese MJ, Lo Celso C *et al.* Hematopoietic stem cell responsiveness to exogenous signals is limited by caspase-3. *Cell Stem Cell* 2008; **2**: 584–594.
80 Laemmli UK. Cleavage of structural proteins during the assembly of the head of bacteriophage T4. *Nature* 1970; **227**: 680–685.
81 Jakel H, Weinl C, Hengst L. Phosphorylation of p27Kip1 by JAK2 directly links cytokine receptor signaling to cell cycle control. *Oncogene* 2011; **30**: 3502–3512.
82 Kalejta RF, Brideau AD, Banfield BW, Beavis AJ. An integral membrane green fluorescent protein marker, Us9-GFP, is quantitatively retained in cells during propidium iodide-based cell cycle analysis by flow cytometry. *Exp Cell Res* 1999; **248**: 322–328.

Supplementary Information accompanies this paper on the Oncogene website (http://www.nature.com/onc)